

Two-dimensional silicon nanomaterials for optoelectronics

Xuebiao Deng, Huai Chen, and Zhenyu Yang[†]

MOE Laboratory of Bioinorganic and Synthetic Chemistry, Lehn Institute of Functional Materials, School of Chemistry, Sun Yat-sen University, Guangzhou 510275, China

Abstract: Silicon nanomaterials have been of immense interest in the last few decades due to their remarkable optoelectronic responses, elemental abundance, and higher biocompatibility. Two-dimensional silicon is one of the new allotropes of silicon and has many compelling properties such as quantum-confined photoluminescence, high charge carrier mobilities, anisotropic electronic and magnetic response, and non-linear optical properties. This review summarizes the recent advances in the synthesis of two-dimensional silicon nanomaterials with a range of structures (silicene, silicane, and multilayered silicon), surface ligand engineering, and corresponding optoelectronic applications.

Key words: two-dimensionality; silicon; nanomaterials; synthesis; surface engineering; optoelectronics

Citation: X B Deng, H Chen, and Z Y Yang, Two-dimensional silicon nanomaterials for optoelectronics[J]. *J. Semicond.*, 2023, 44(4), 041101. <https://doi.org/10.1088/1674-4926/44/4/041101>

1. Introduction

Two-dimensional (2D) materials have attracted immense attention and interest from the scientific community and industry. By definition, 2D materials refer to laterally infinite and ordered structures with a thickness within single or several atoms. Differing from their three-dimensional (3D) bulk counterparts, materials with 2D layered, anisotropic structures have many compelling physical and chemical properties such as dimensional confinement of charge carriers, anisotropic electronic and magnetic response, non-linear optical properties, superior mechanical strength and flexibility, and facet-dependent catalytic behaviors^[1–5]. With these features, 2D materials have shown great promise in a number of applications, such as energy storage^[6–9], optoelectronics^[10, 11], and artificial neural devices^[12–15].

Graphene, the carbon allotrope in a monolayer with a planar structure and has undoubtedly been the center of 2D material research in the last decade. Other Group 14 elements, such as silicon and germanium, have also gained considerable attention because of the similarity of their electronic structure compared to graphene based on theoretical calculations^[16]. It is also believed that 2D silicon (2DSi) may be one of the material candidates to substitute crystalline silicon (c-Si) for the next-generation electronics. To date, the materials properties of 2DSis have been widely investigated through both experimental and computational studies^[16–25]. The corresponding optoelectronic features of 2DSis have been described in simulation reports, such as size-tunable electronic structures and direct-bandgap-like electronic structures^[26, 27]. These remarkable properties enable 2DSis to be considered as candidates for active materials in various optoelectronic devices, such as light-emitting diodes (LEDs), and photodetectors^[28–32].

To date, despite a vast number of reports about the simu-

lated properties of 2DSi nanostructures, there have only been a few experimental results focusing on the synthetic approaches and the material characterizations of 2DSis. One of the major reasons for this gap is the relatively complex procedures for the preparation of 2DSis. Unlike graphene, which can be prepared using numerous chemical and physical approaches (e.g., mechanical exfoliation, electrochemical synthesis, hydrothermal assembly, etc.), there are only a few synthetic routes to make 2DSis with clear structures^[33–35]. Meanwhile, inconsistent results about the physical and chemical properties of 2DSis are commonly found in the literature, including experimental studies and theoretical predictions. It is therefore important to summarize the results from both experimental and theoretical studies for deepen the understanding of the chemical and physical properties of 2DSi. Therefore, in this review article, we aim to provide a comprehensive summary of the recent development in the research field of 2DSi nanomaterials, especially focusing on the progress of synthesis, surface functionalization, and the corresponding optoelectronic applications.

The contents of this review are divided into four major sections. The discussion starts with a description of the various types of 2DSi materials (the first section) and the general synthetic protocols (the second section). In the third section, we describe several surface functionalization approaches to chemically modify the surface of 2DSis, which improve the chemical and physical properties of the intrinsic layered silicon backbones. The discussion in the fourth section focuses on the electronic properties and the state-of-the-art optoelectronics based on 2DSi materials. We sought to connect the structural properties and the surface bonding environments of various types of 2DSis with their optoelectronic behaviors and device performance. We finally provide some viewpoints on the future directions of the field of 2DSi-based optoelectronics.

2. Crystallinity and electronic structures of two-dimensional silicon

There may be a misconception that 2DSi is a new mem-

Correspondence to: Z Y Yang, yangzhy63@mail.sysu.edu.cn

Received 23 SEPTEMBER 2022; Revised 7 NOVEMBER 2022.

©2023 Chinese Institute of Electronics

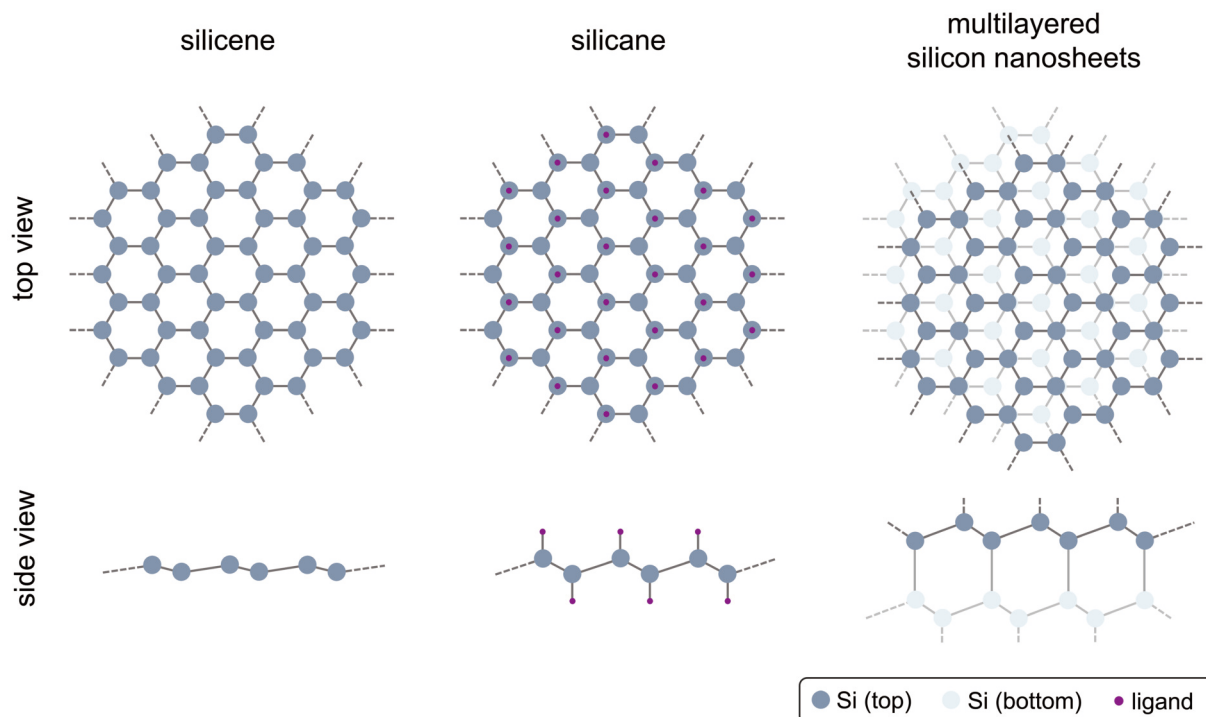


Fig. 1. (Color online) Schematic illustration of three types of 2D silicon nanomaterials. Silicene refers to the monolayered hexagonal lattice with sp^2 - sp^3 hybridized Si atoms; silicane refers to the monolayered hexagonal lattice with sp^3 hybridized Si atoms fully or partially passivated by ligands such as hydride, hydroxyl, alkyl groups; multilayered silicon nanosheet refers to the diamond-structured silicon with a thickness of a few atomic Si layers.

ber of the 2D material family, although the immense discussion about 2DSi only arises after the discovery of graphene^[36]. The finding of silicon with layered structures was first reported by Wöhler *et al.* in 1863^[37]. It was noticed that yellow-green-colored sheet-like powders could be obtained when calcium silicide ($CaSi_2$) is mixed with concentrated HCl solution. It was later confirmed that the product was partially hydroxylated silicane ($Si_6H_3(OH)_3$)^[38, 39]. According to the definition, there are three types of 2DSis whose terms have been widely used in literature: silicene, silicane, and multilayered silicon nanosheets. Because these structures are highly relevant and may cause potential confusion, we summarize their structural features in Fig. 1.

2.1. Silicene

Silicene is a two-dimensional allotrope of silicon whose structure is similar to that of graphene. In contrast to the graphene-like flat 2D structure, silicene has a monolayered hexagonal structure but buckled to tiny degrees (Fig. 1). This happens because the Si atoms in silicene tend to adopt mixed sp^x hybridization, where $2 < x < 3$. Based on the results from computational studies, the energy difference of mixed hybridized (i.e., sp^2 - sp^3) silicene with a buckle-like structure is much more stable than the planar counterpart^[16]. The in-plane lattice constant of 6.4 Å was measured experimentally from the silicene sample grown on an Ag(111) structure under ultrahigh vacuum (UHV) conditions^[29]. Because silicon atoms favor the sp^3 hybridization to construct the Si-Si-bond-based network, it is not unexpected that silicene is not stable against air or moisture; indeed, there is no report about the successful preparation of freestanding silicene under those conditions.

The partially conjugated structures enable silicene to have a similar electronic structure to that of graphene. For instance, it has been predicted that silicene also has a Dirac cone, and the charge carriers within may behave like Dirac fermions at the K point^[16]. Silicene also shows linear electronic dispersion at the regimes close to the Dirac points with a calculated Fermi velocity value of 5.1×10^5 m/s^[17]. Meanwhile, the slightly buckled structure enables silicene to have a more substantial quantum spin Hall effect than graphene. Based on the first-principle calculations, the Dirac point in silicene is expected to be opened at low temperatures due to the strong spin-orbit coupling^[19]. Because the transition temperature of 18 K is much higher than that of graphene (below ~ 0.01 K)^[40], the bandgap of silicene can be further tuned by the application of an external inhomogeneous electric field (the critical electric field is around 17 mV/Å)^[41]. These features suggest that silicene can be applied to spintronic devices under more realistic operational conditions.

2.2. Silicane

Although it is commonly misnamed as “silicene” in the literature^[42], silicane is another class of 2DSi in which silicon atoms are fully sp^3 hybridized (Fig. 1). Unlike the sp^2 -based framework of silicene, silicon atoms on silicane are passivated by adatoms or organic groups to maintain sp^3 hybridization. Because of the additional surface passivating groups, silicane cannot be considered as the allotrope of silicon. Various names have been given for silicane structures with different surface passivants (e.g., siloxene ($Si_6H_3(OH)_3$), layered polysilane (Si_6H_6)) to distinguish them from their linear polysilane counterparts, which are mostly synthesized from the dehydrogenative coupling or Wurtz-type reductive dehalogenation re-

actions^[43].

Regardless of different passivating ligands, the buckled silicon backbone within silicane is similar to the (111) facet of crystalline silicon (c-Si). The Si–Si bond length is ~ 2.35 Å^[39], which is the same as that in c-Si. The lateral distance between two adjacent silicane sheets varies from 0.59 nm up to 3 nm depending on the type of passivating ligand^[39, 44, 45]. However, the electronic structure is insensitive to the length of the ligands^[45]. This happens because the valance band (VB) maximum energetic states and the conduction band (CB) minimum energetic states are dominated by the contribution of the silicon atoms^[45]. Ryan *et al.* investigated the band structure of silicane with OH- and Cl-terminating groups and showed similar band structures and projected density of states (pDOS) compared to previous reports^[27]. The density functional theory (DFT) simulation results also confirmed the “direct-like” bandgap behavior of silicane (direct bandgap: 2.26 eV, indirect bandgap: 2.16 eV). It was also predicted that the surface-terminated elements with larger electronegativity values may cause the downshifting of the bandedge compared with that of H-terminated silicane^[27].

2.3. Multilayered silicon nanosheets

Multilayered silicon nanosheets (MSNs) are representative 2DSi nanostructures with a thickness greater than one but less than tens of silicon atomic layers. MSNs with various structures have been investigated through computational studies^[22]. However, only two general structures have been experimentally determined: (I) multilayered silicene and (II) ultrathin diamond-like c-Si^[46]. These two structures can be distinguished through spectroscopic and microscopic techniques such as Raman spectroscopy^[47], energy dispersive grazing incidence X-ray diffraction (ED-GIXRD), and scanning tunneling microscopy (STM)^[48]. While the former is only found from the sample prepared by the epitaxial growth approaches^[49], the 2D structure with intrinsic c-Si scaffold can be prepared by multiple synthetic methods such as solution-based wet chemistry methods or vapor-deposition-based techniques^[50].

It has been theoretically predicted that multilayered silicene has linearly dispersed Dirac bands^[51], similar to that present in the bilayered graphene^[22]. The presence of Dirac fermions has been experimentally confirmed by spectroscopic techniques such as angle-resolved photoelectron spectroscopy and scanning tunneling spectroscopy (STS)^[52, 53]. Computational results also reveal that the band structures and the doping properties of ultrathin c-Si nanosheets with double-layered diamond structures are highly tunable and dependent on the surface terminating groups^[18].

Due to the incorporation of mixed sp^2/sp^3 hybridization of silicon atoms within the constitutive multilayered backbone, the structural transfer between the multilayered silicene and the ultrathin c-Si can occur under relatively high temperatures (e.g., 200–300 °C)^[46, 47], which can be monitored by STS and Raman spectroscopy. It has also been noticed that the ultrathin c-Si structure (i.e., cubic structured silicon nanosheet) experiences an irreversible phase transition (cubic \rightarrow tetragonal \rightarrow hexagonal) during the increase of pressure, and finally forms one-dimensional (1D) c-Si nanowires^[54]. The corresponding computational studies have further indicated the reduction of thermal conductivity in such 1D structures, which may allow the application of these ultrathin structures in thermoelectric devices.

3. Preparation of 2D silicon nanomaterials

Despite the existence of numerous 2D models in theoretical studies, only a few structures of 2DSi have been successfully synthesized with comprehensive analyses of the crystal structures. There are some excellent reviews that have summarized detailed experimental conditions to prepare 2D silicon materials^[50, 55, 56]. In this review, we prefer the description of the formation mechanisms within those synthetic protocols.

As for graphene, the typical 2D structures of elemental carbon can be directly synthesized by the exfoliation of graphite^[36]. However, 2DSi cannot be obtained from the physical exfoliation of c-Si because of the strong covalent backbone of the diamond structure. Nowadays, there are two general approaches to preparing 2D silicon nanomaterials: epitaxial growth and chemical exfoliation (Fig. 2).

The preparation of silicene is achieved via the epitaxial growth approach. Generally, freestanding silicon atoms are first generated by the pyrolysis of silicon precursors (e.g., silanes) or the ionization of bulk silicon under high current (e.g., > 90 A)^[57, 58], which are subsequently deposited on specific substrates (e.g., Ag(111)^[29, 59], Ir(111)^[60], and ZrB₂(0001)^[61]. The high crystalline coherence between the graphene-like honeycomb lattice structure of silicon and the predesigned inorganic phase of the substrate allows the alignment of silicon atoms and forms planar silicene via heterointerface with the substrate. It is important to note that silicene is extremely reactive with oxidants due to the unstable sp^2 -hybridization of silicon. Consequently, the preparation and characterizations of silicene are required to be performed under UHV conditions. Combined with the computational structural analysis, atomically resolved STM is a powerful tool to reveal the epitaxially grown silicene structures^[23, 59]. Feng *et al.* reported the experimental results of silicene sheets grown on Ag(111) surfaces. The line-scan profiles analysis revealed a height difference of 0.2 Å between two adjacent layers of silicon atoms, indicating Si sp^2 - sp^3 hybridization, which aligns well with the theoretical prediction^[29].

Chemical exfoliation is a “top-down” strategy that has been widely used in the preparation of materials with layered structures^[62–64]. Chemical exfoliation is also the first recorded method to prepare 2DSi. In 1863, Wöhler *et al.* mixed calcium silicide (CaSi₂) with concentrated HCl aqueous solution and obtained yellow-green colored sheet-like powders, which were later confirmed to be partially hydroxy-terminated silicane (Si₆H₃(OH)₃)^[37–39]. It is widely accepted that metal silicide precursors (e.g., CaSi₂, MgSi₂) with layered structures are key to preparing silicane sheets with various terminating groups. These metal silicides share Si₆ cyclohexane-like subunits interconnected in each plane separated by a bivalent cation layer (Fig. 2(b)). The liberation of a single layer of silicon can be achieved by the deintercalation of bivalent metal cations during the hydrogenation reaction^[65].

The reaction parameters are crucial to the preparation of silicane. Yamanaka *et al.* reported that low synthetic temperatures (e.g., below –30 °C) could effectively inhibit the surface oxidation of as-formed Si–H surfaces, yielding hydride-terminated silicane^[65]. Once the temperature increases to 0 °C, the oxidation becomes evident, yielding silicanes with mixed hydride/hydroxide termination^[65]. The size of silicane can be fur-

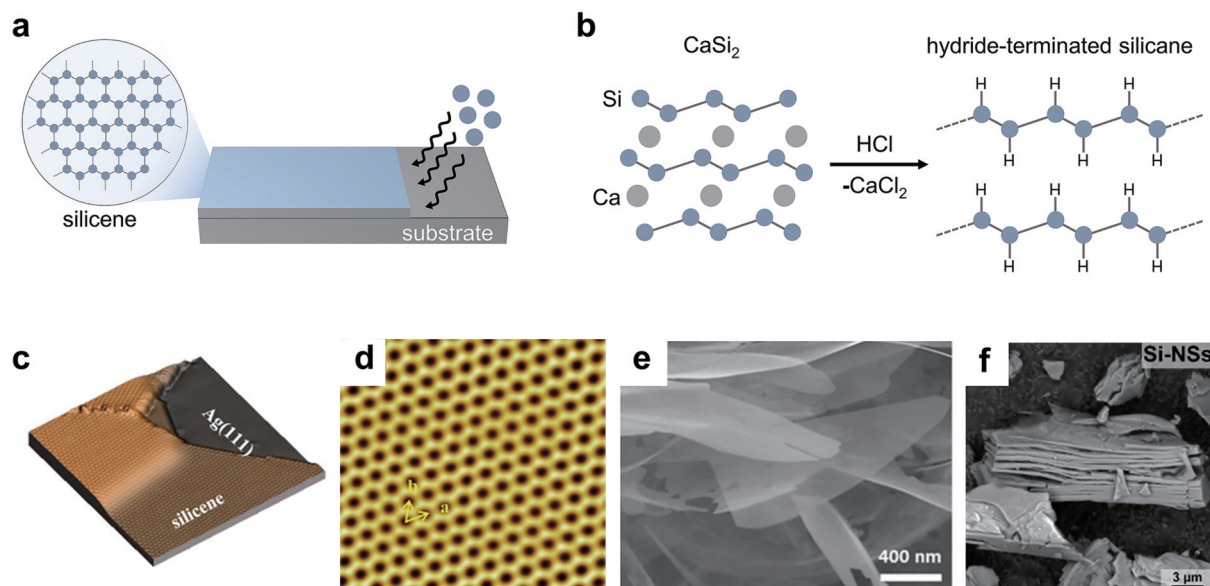


Fig. 2. (Color online) Preparation of 2D silicon nanomaterials. (a, b) Schematic illustration of two general synthetic approaches: epitaxial growth and chemical exfoliation. (c) STM image of a single-layered silicene island on Ag(111). (d) High-resolution STM image of monolayer silicene terrace showing the $\sqrt{3} \times \sqrt{3}$ honeycomb superstructure. Reprinted with permission from Ref. [29]. Copyright 2012 by American Chemical Society. (e) Scanning electron microscopic (SEM) images of freestanding MSNs prepared using the epitaxial growth method. Reprinted with permission from Ref. [30]. Copyright 2014 by American Chemical Society. (f) SEM image of layered silicane obtained from the chemical exfoliation of CaSi_2 . Reprinted with permission from Ref. [27]. Copyright 2020 by American Chemical Society.

Table 1. Summary of recently reported approaches to prepare 2DSi nanomaterials. Note: EG = epitaxial growth, CE = chemical exfoliation.

Product	Year	Synthetic method	Silicon source	Lateral size (μm)	Thickness (nm)	Ref.
Silicene	2012	EG on Ag(111)	Si wafer	>0.03	–	[29]
Silicene	2013	EG on Ir(111)	Si wafer	>0.02	0.06	[60]
Silicane	2006	CE of metal silicide	$\text{CaSi}_{1.85}\text{Mg}_{0.15}$	0.2–0.5	0.37	[66]
Silicane	2018	CE of metal silicide	CaSi_2	~3.7	0.6	[42]
MSN	2014	EG on Si substrate	SiCl_4	–	1–13	[30]
MSN	2014	Arc discharge	bulk Si	0.02	2.4	[57]
MSN	2017	EG on Ag(111)	Si wafer	>0.05	7	[47]
MSN	2017	CE of metal silicide	$\text{Li}_{13}\text{Si}_4$	~5.1	4	[67]
MSN	2018	EG on NaCl substrate	SiH_4	~5.2	50	[58]

ther tailored by the reaction time. Mixed hydride/hydroxide-terminated silicane with a size up to $\sim 0.25 \mu\text{m}^2$ can be formed from a prolonged reaction (e.g., up to 10 days) at room temperature^[66].

Both epitaxial growth and chemical redox reactions can be utilized to prepare multilayered silicon nanosheets. Despite the difference in thickness and morphology, silicon nanosheets share a similar cubic diamond crystal structure and thus can be readily prepared using the epitaxial growth approach. Dong *et al.* reported the formation of freestanding silicon nanosheets by depositing silicon atoms on a water-cooled wall of the evaporation chamber at high discharge voltage under a slightly reducing atmosphere^[57]. The redox reactions of metal silicides can also form a multilayered structure. In this case, metal silicide precursors may not contain the closely packed layer of silicon atoms. For instance, lithium silicide ($\text{Li}_{13}\text{Si}_4$) with an orthorhombic structure can be converted to layered silicon nanosheets while leaching in ethyl alcohol and thermal annealing at 550°C ^[67].

The optimization of synthetic parameters enables the structural conversion of 2DSi. Grazianetti *et al.* demonstrated that both multilayered, stacked silicene and diamond-structured

silicon nanosheets were formed by the epitaxial growth of silicon on an Ag(111) substrate at temperature regimes^[47]. Single-layered silicene can be used as the template or precursor for the growth of the successive layer with a thickness of up to 24 layers of silicon atoms. *In situ* STM analysis and Raman spectroscopic results indicated the formation of multilayered silicene and diamond-structured silicon at intermediate ($200\text{--}230^\circ\text{C}$) and high (350°C) temperature regimes, respectively. The sp^2 -hybridized silicon atoms in silicene can be converted to partially sp^3 -hybridization under hydrogenation, yielding a “half-silicane” structure whose sublattice is fully hydrogen-saturated and the other lattice is intact due to the direct contact with the Ag(111) substrate^[68, 69]. Table 1 summarizes recent progress in the preparation of 2DSi materials and the corresponding synthetic features.

4. Surface modification of 2DSi

Similar to other silicon-based nanostructures, the as-formed 2DSi materials are prone to oxidation^[70, 71]. As for silicene, the backbone is constructed by the sp^2 - sp^3 network of silicon with partially dangling bonds. Therefore, the surface silicon atoms on silicene are supposed to be “naked”, and the sili-

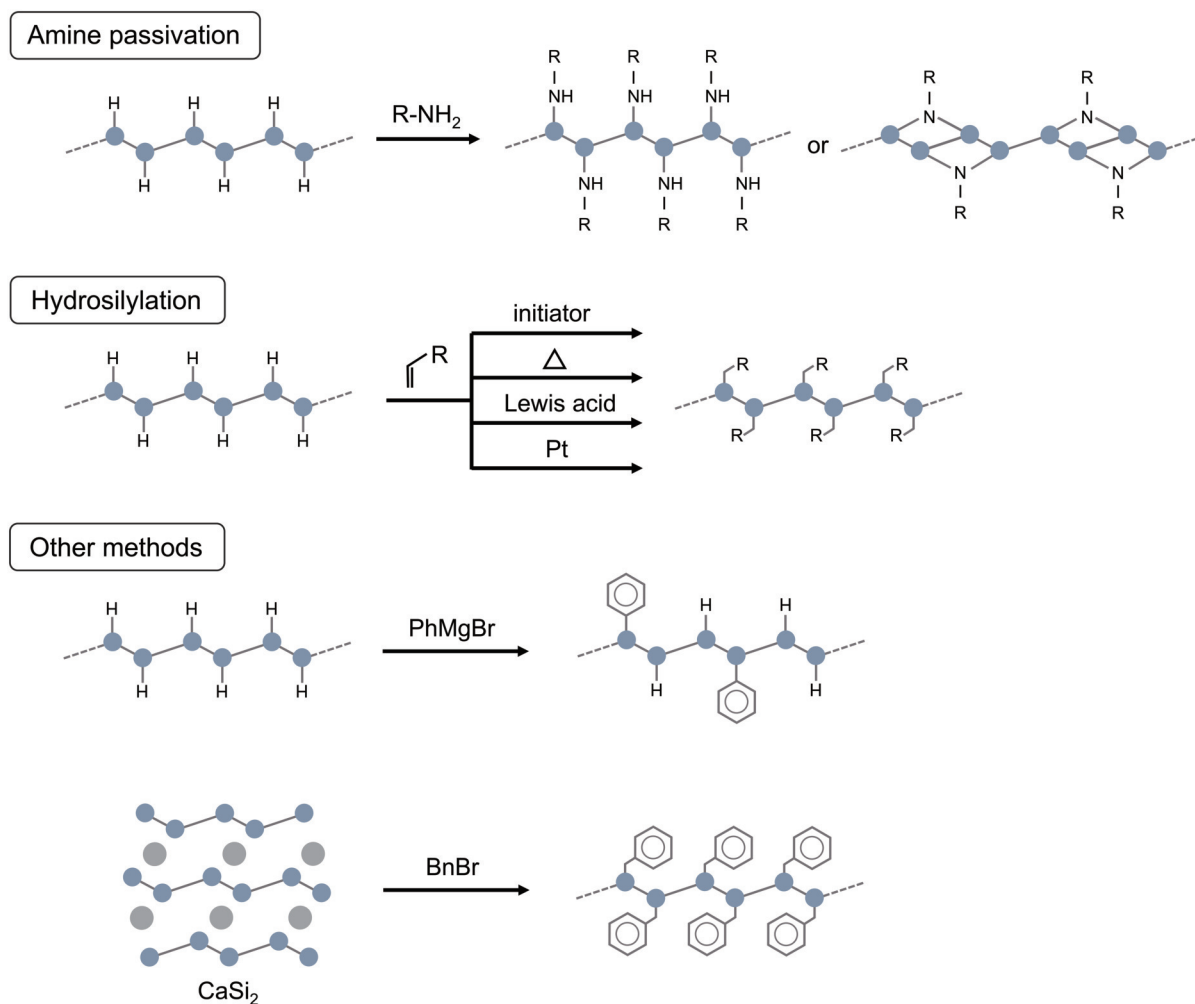


Fig. 3. (Color online) Schematic illustration of some recently reported surface modification approaches of 2DSi. R = alkyl/aryl group; Ph = phenyl; Bn = benzyl.

cene's pseudo-planar structure is only stable under UHV conditions^[72]. The post-synthetic passivation of the silicon atoms with sp^2 -hybridization or dangling bond structures causes the reconstruction of silicene, yielding half- or full-silicene with various terminating groups^[68, 69]. In contrast, surface modification does not change the hybridization of silicon atoms in silicene and multilayered silicon nanosheets. Consequently, the discussion in this section only focuses on sp^3 -hybridized 2DSi structures.

The as-formed silicene and multilayered silicon nanosheets are mostly terminated by either hydride or hydroxyl groups, regardless of the synthetic process used. Because of the weaker binding energy compared to that of the Si–O bond (Si–H: 318 kJ/mol, Si–O: 452 kJ/mol)^[73], the surface Si–H bonds are inevitably oxidized when 2DSi materials are exposed to air or moisture atmosphere. The non-controllable oxidation^[27] cleaves the Si–Si bonds and forms Si–O–Si connections^[74]. The reactions involving the adjacent layers of silicenes further destroys the original stable layered structure, and turn into an irregular amorphous silicon structure^[8].

It is highly possible that the oxidation of silicon introduces surface trap states and impair the optical properties of silicene. Consequently, it is crucial to apply surface modification approaches to stabilize the 2DSis and inhibit the formation of undesired electrical/optical traps. The general reactivity of Si–H bonds on 2DSi is similar to those on the molecu-

lar silanes, bulk c-Si, and Si nanocrystals, although the bond strength may slightly vary due to the difference in steric hindrance on these structures. Various procedures have been developed for passivating silicon surfaces which have been demonstrated to functionalize 2DSis. This section reviews several strategies to modify the surfaces of hydride-terminated 2DSi with robust chemical bonds such as Si–O, Si–C, and Si–N. Some recently reported surface modification approaches and related benefits are summarized in Fig. 3.

4.1. Amine passivation

Organoamines can directly react with hydride-terminated silicon surfaces due to their nucleophilic nature, yielding stable Si–N covalent bonds^[75]. The observation of amine-passivation on 2DSi was first reported by Okamoto *et al.* and gave well-defined layered structural organoamine-functionalized surfaces (Fig. 4)^[44]. Hydride-terminated silicene prepared at low temperature reacts with decylamine at 60 °C for 12 h under an inert atmosphere, yielding stacked, amine-functionalized silicene. Similar to silicon nanocrystals (SiNCs), the interaction between silicene with nitrogen source leads to size-independent blue photoluminescence (PL) at 450 nm, which was assigned to the trap-induced radiative recombination^[75]. The surface modification of SiNCs using amine sources is usually incomplete and introduces a substantial amount of oxide species^[75]. However, the oxidation was not found from the

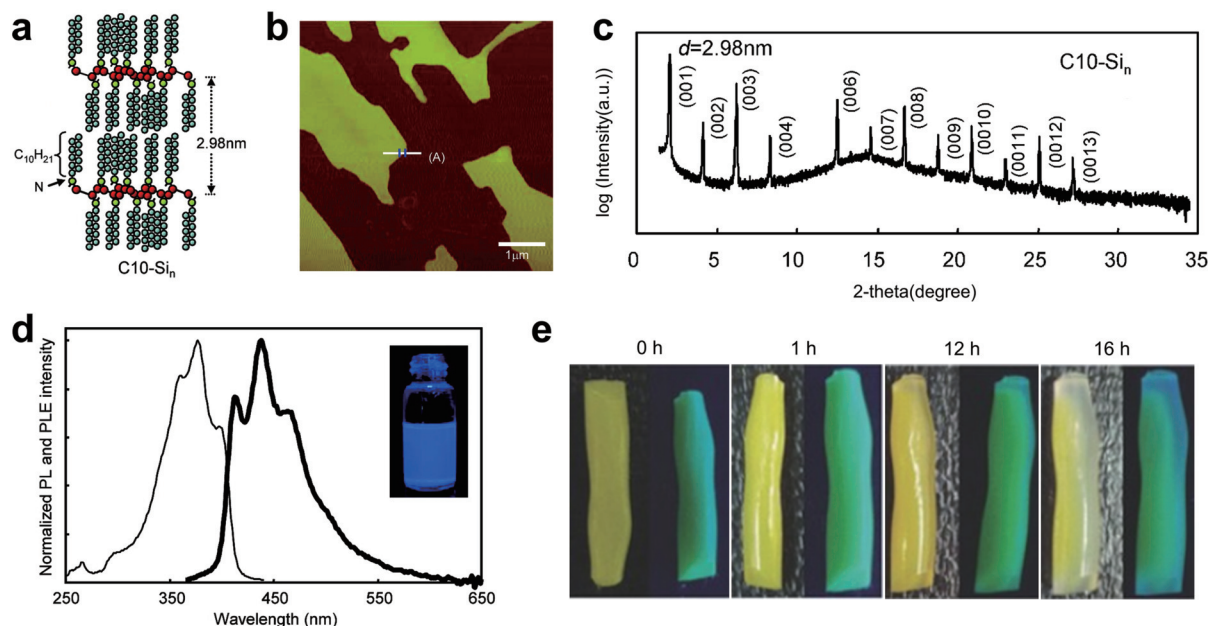


Fig. 4. (Color online) Material properties of surface-modified 2DSis. (a) Structural models of regularly stacked ($C_{10}\text{-Si}_n$). (b) AFM phase image of decylamine-functionalized silicane ($C_{10}\text{-Si}_n$) on a highly oriented pyrolytic graphite plate. (c) X-ray diffraction (XRD) pattern of $C_{10}\text{-Si}_n$ with strong signals corresponding to the layered structure of silicane. (d) PL spectrum of the amine-passivated silicane. Reprinted with permission from Ref. [44]. Copyright 2010 by American Chemical Society. (e) Hybrid materials containing silicanes and polymers shows enhanced materials stability and PL property under continuous UV irradiation. Reprinted with permission from Ref. [77]. Copyright 2016 by Wiley-VCH.

amine-passivated silicane as indicated by spectroscopic techniques such as Fourier-transform infrared (FT-IR) spectroscopy and X-ray absorption near-edge structure (XANES) analysis[44].

Ohshita *et al.* further demonstrated that the single-step amine-functionalization approach could effectively link silicane with aromatic substituents[76]. Three types of aromatic organoamines (benzylamine, 1-naphthylmethylamine, and (9-Butyl-9H-carbazol-3-yl)-methanamine) can directly substitute the original Si-H bonds, yielding arylmethylamine modified 2DSi. The additional absorption features and excitation-dependent PL features suggest that arylmethylamine-ligands with expanded conjugation affect the optical properties of 2DSi.

4.2. Hydrosilylation Reactions

Hydrosilylation is a class of reactions of Si-H bonds with unsaturated organic groups (e.g., alkenes, alkynes) to form robust Si-C bonds. Because hydrosilylation strategies provide effective passivation of silicon atoms, they have been widely applied to stabilize and modify silicon surfaces. Linford and Chidsey reported the first example of hydrosilylation on the surface of bulk silicon in 1993[78]. Since then, several proposed mechanisms have been proposed, such as homolytic cleavage of the Si-H bond[79–82], exciton mediation[83], radical-driven Si-H cleavage[84], and photoemission[85]. Many of these hydrosilylation approaches have been applied to modify Si-H bonds on 2DSis, with very few exceptions. For instance, Helbich *et al.* observed that the 2D features and the PL of silicon nanosheets disappear after the UV irradiation[77]. This result indicates that the 2DSi material is sensitive to the light irradiation and thus photoinitiated hydrosilylation reactions (e.g., photoinitiated Si-H cleavage, exciton mediation) should not be applied on 2DSis.

Homolytic cleavage of Si-H bonds on 2DSi and the sub-

sequent hydrosilylation reactions can be driven by heat or radical initiators under mild conditions. Thermal hydrosilylation is one of the most commonly used hydrosilylation approaches to functionalize silicon surfaces (Fig. 5). It is efficient, catalyst-free, and morphologically independent, and has been examined to be effective to functionalize hydride-terminated silicane with functional alkenes and alkynes[86, 87]. Commercially available radical initiators (e.g., decylbenzene diazonium tetrafluoroborate (DDB) and azobisisobutyronitrile (AIBN))[77, 86] have been proven to effectively initiate the hydrosilylation reactions on 2DSi at relatively low temperatures, yielding functionalized 2DSi and even 2DSi/polymer hybrid materials (Fig. 4(f))[77, 88, 89].

Lewis acids are capable of initiating hydrosilylation reactions on molecular silanes[90], bulk *c*-Si[91], and colloidal SiNCs[92]. Similar approaches have also been applied on 2DSis to prepare inorganic/organic hybrid thin films[93]. Helbich *et al.* reported a series of organoboranes that can effectively cleave the Si-H bonds on 2DSis and enable subsequent functionalization with unsaturated organic molecules (Fig. 5)[93].

4.3. Alternative functionalization approaches

The Grignard-based protocol to the surface modification of silicon nanostructures is drawn from its molecular silane analogues. A two-step approach to passivate surface Si-H bonds has been proposed: (i) halogenation to convert surface Si-H bonds to Si-X bonds (X = halide groups, such as Cl, Br); and (ii) subsequent reaction with Grignard reagents to form alkyl-terminated surfaces. Following the idea of Grignard reactions, Sugiyama *et al.* proposed to functionalize silicane using phenyl magnesium bromide as the Grignard reagent[94]. Interestingly, the modification was even achieved by a single-step reaction between hydride-terminated 2DSi and the Grignard reagent, indicating that the Si-H bonds on silicane have higher reactivity than those on bulk *c*-Si or silicon nanocrystals.

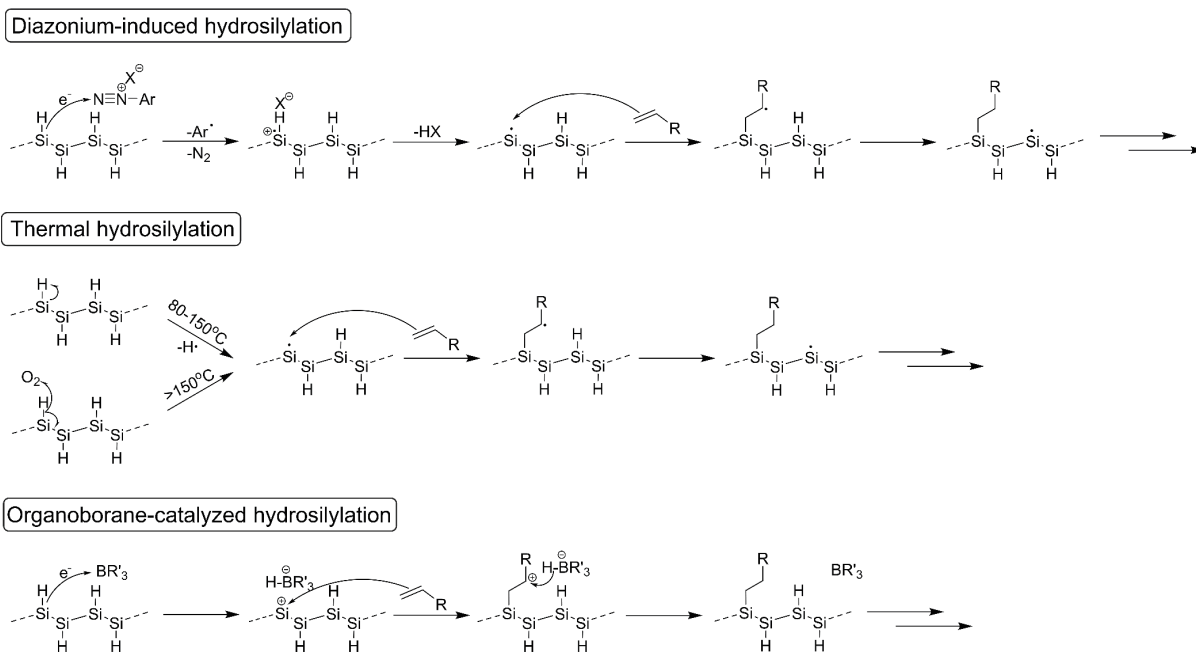


Fig. 5. Proposed mechanisms of the hydrosilylation reaction on 2DSi^[86, 93].

However, due to the large steric hindrance of the phenyl ring, the substitution from hydrogen to phenyl group was not complete, yielding partially phenyl-passivated silicene with intense blue emission (Fig. 6(a)).

Ohashi *et al.* also demonstrated a direct surface modification approach on 2DSi using benzyl bromide as the passivant and the solvent^[95]. The nucleophilic reaction between calcium silicide and benzyl bromide can occur at 150 °C in a sealed Teflon reactor, in which the benzyl-passivation on Si atoms proceeded in parallel with the cleavage of CaSi₂. The introduction of the surface benzyl group leads to the shrinkage of the bandgap, resulting in the red-shift of the absorption edge of the functionalized 2DSi (Fig. 6(b)).

5. Optoelectronic properties and applications

As a new member in the 2D material family and a silicon allotrope in ultrathin structure, 2DSi may pave the way for silicon in diverse applications such as lithium-ion battery anodes^[42, 96], sensors^[97, 98], photocathode^[99], and catalysis^[100]. 2DSi have also been considered for use as active materials in electronic devices due to their unique fundamental features such as indirect-bandgap-like band structures^[27], quantum spin Hall effect^[19], chiral superconductivity^[101], and exotic field-dependent states^[102]. In the following section, we focus on the recent computational and experimental advances in 2DSi-based optoelectronics.

5.1. Theoretical input

Theoretical studies have predicted that the charge carriers on sp²-hybridized silicene would have massless particles due to the linear Fermi–Dirac dispersion from the half-filled p_z orbitals^[16]. Unlike graphene, silicene has a smaller bandgap (around 1.55 eV) opening at the Dirac point^[19], and the Fermi velocity extracted from the Dirac cone is around 5.8 × 10⁷ cm/s^[103]. It has also been predicted that silicene will exhibit extremely high electron mobility. The calculation results by Kim *et al.* indicate that the intrinsic mobility of silicene is ~1200 cm²/(V·s) with a saturation velocity of 3.9 × 10⁶ cm/s

at 300 K (Fig. 7(a))^[103]. The bandgap and carrier mobility can be further tuned by adjusting dopant elements, surface modification, and defects. Ding *et al.* investigated the bandgap structures of hydride- and fluoride-passivated silicene (H-silicene and F-silicene) and showed that the surface adatoms could significantly change the band structure (H-silicene: indirect bandgap, E_g = 2.19 eV; F-silicene: direct bandgap, E_g = 0.70 eV)^[104]. The bandgap modification can also be achieved by the attachment of organic ligands such as alkyl-, alkoxy-, and amine-groups (Figs. 7(b)–7(g))^[45, 105]. The high tunability of band structure makes 2DSi an attractive, active material for transistor applications. In 2012, Ni *et al.* investigated the functions of 2DSi-based FETs and showed that dual-gated silicene has a low on-off ratio of 4.2 when applying a vertical electric field of 1 V/Å at 300 K^[106]. Quhe *et al.* noted that sodium adatoms can effectively increase the bandgap of 2DSi, which substantially improves the on-off ratio of 2DSi-based FETs up to 4 × 10⁸^[26].

5.2. Photocurrent response

The light-induced photocurrent of silicene was first analyzed by Sugiyama *et al.* in the report about phenyl passivation on silicene via the Grignard reaction approach^[94]. The phenyl-capped silicene (Si₆H₄Ph₂) sample was drop-cast on a SnO₂-F (FTO) substrate and used as the photoelectrode in a photoelectrochemical cell. The photocurrent was detected when the electrode was directly irradiated using a xenon lamp and disappeared when the irradiation was discontinued, indicating that the photocurrent forms via a bandgap transition.

The photoexcitation wavelength depends on the absorption band edge; therefore, it is crucial to tailor the absorption range of 2DSi. Ohshita *et al.* observed that the capping ligands with extended conjugating features (e.g., naphthylmethyl and carbazolylmethyl groups) could introduce additional absorption features and facilitate the photocurrent generation^[76]. This phenomenon was found from the benzyl-passivated silicene sample as the bandgap of silicene re-

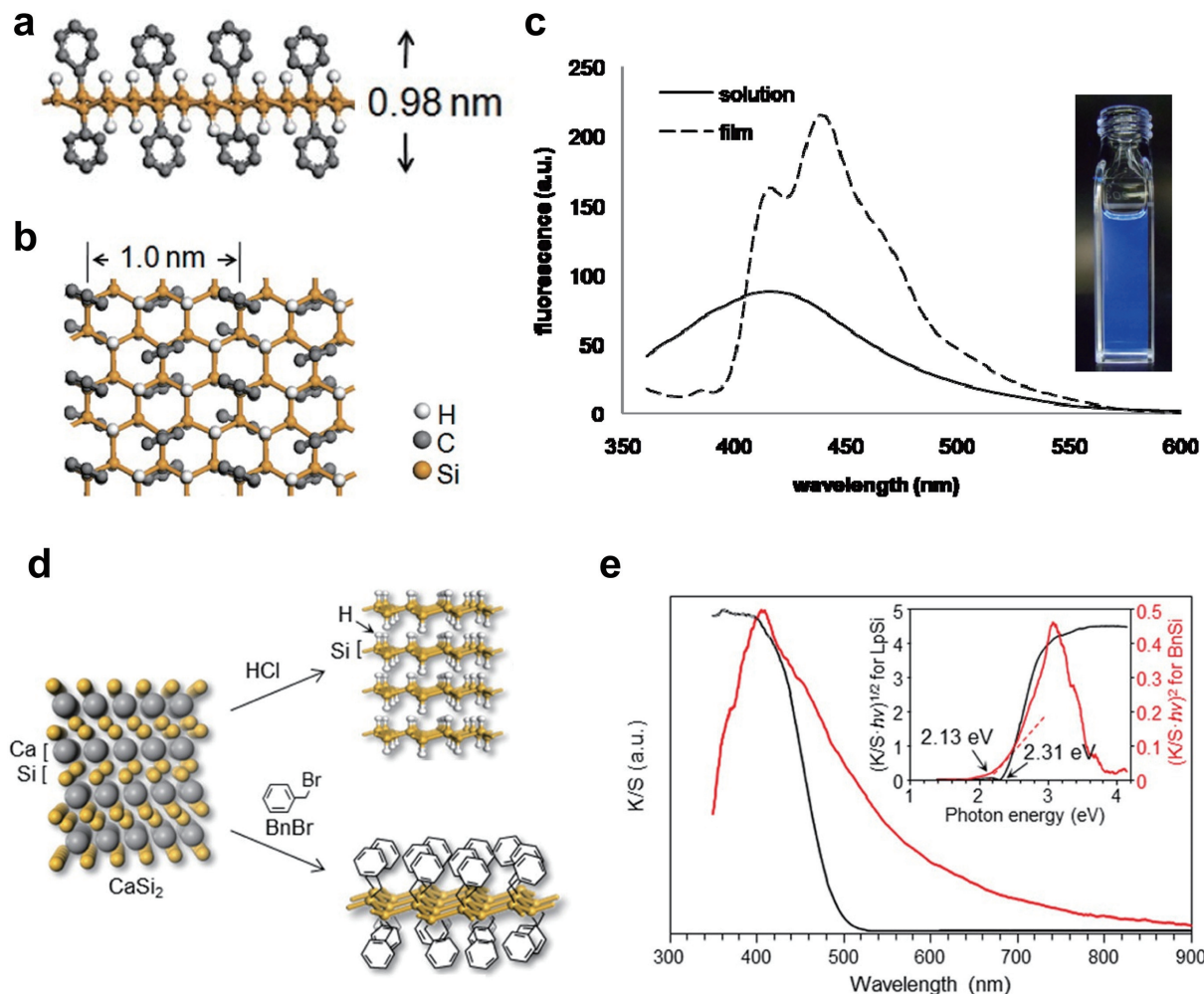


Fig. 6. (Color online) Surface modification of silicenes using single-step approaches. (a) Side view and (b) top view of the model structure of silicene partially passivated by hydride and phenyl groups ($\text{Si}_6\text{H}_4\text{Ph}_2$). (c) PL spectra of $\text{Si}_6\text{H}_4\text{Ph}_2$ thin film and solution (solvent: 1,4-dioxane, excitation wavelength: 350 nm). Inset: blue emitting $\text{Si}_6\text{H}_4\text{Ph}_2$ dispersed in 1,4-dioxane under 365 nm UV irradiation. Reprinted with permission from Ref. [94]. Copyright 2010 by American Chemical Society. (d) Hydride- and benzyl-passivated silicene directly made by the solvent-assisted chemical exfoliation of CaSi_2 (e) Diffuse reflectance spectra of hydride-passivated (black) and benzyl-passivated 2DSi (red). Inset: Tauc plots of both 2DSi samples. Reprinted with permission from Ref. [95]. Copyright 2019 by American Chemical Society.

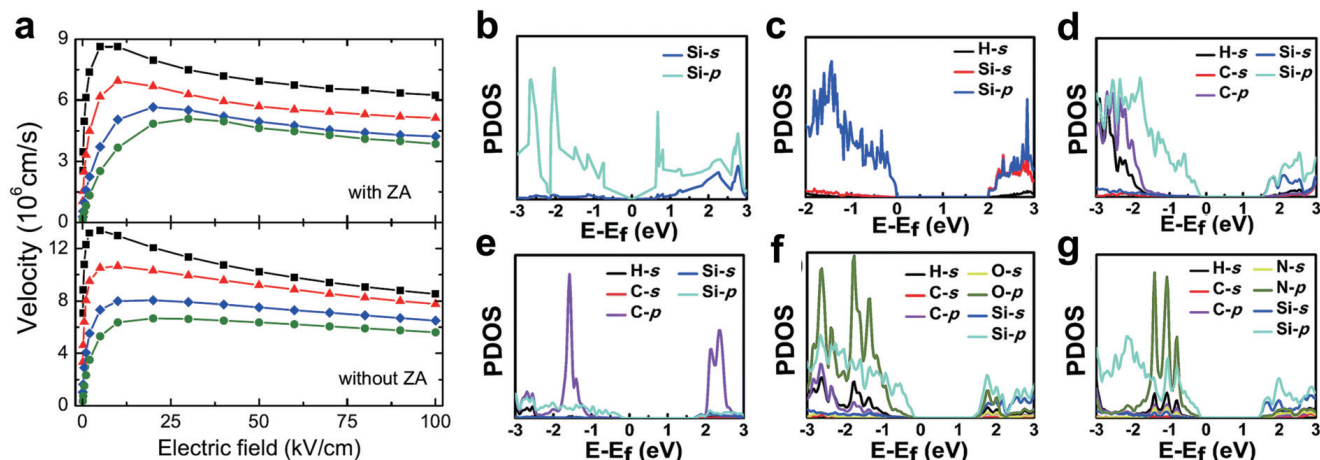


Fig. 7. (Color online) Electronic structures of pristine and surface-modified silicene. (a) Monte Carlo simulation results of temperature-dependent drift velocity behaviors of monolayer silicene (with or without out-of-plane acoustic (ZA)): 50 K (square), 100 K (triangle), 200 K (diamond), and 300 K (circle). Reprinted with permission from Ref. [103]. Copyright 2013 by American Physical Society. (b–g) The partial density of states of various types of surface-modified silicene: (b) pristine (i.e., “naked”) silicene, (c) hydride-terminated silicene, (d) hydrosilylated silicene, (e) phenylated silicene, (f) alkoxyated silicene, and (g) aminated silicene. Reprinted with permission from Ref. [105]. Copyright 2015 by Royal Society of Chemistry.

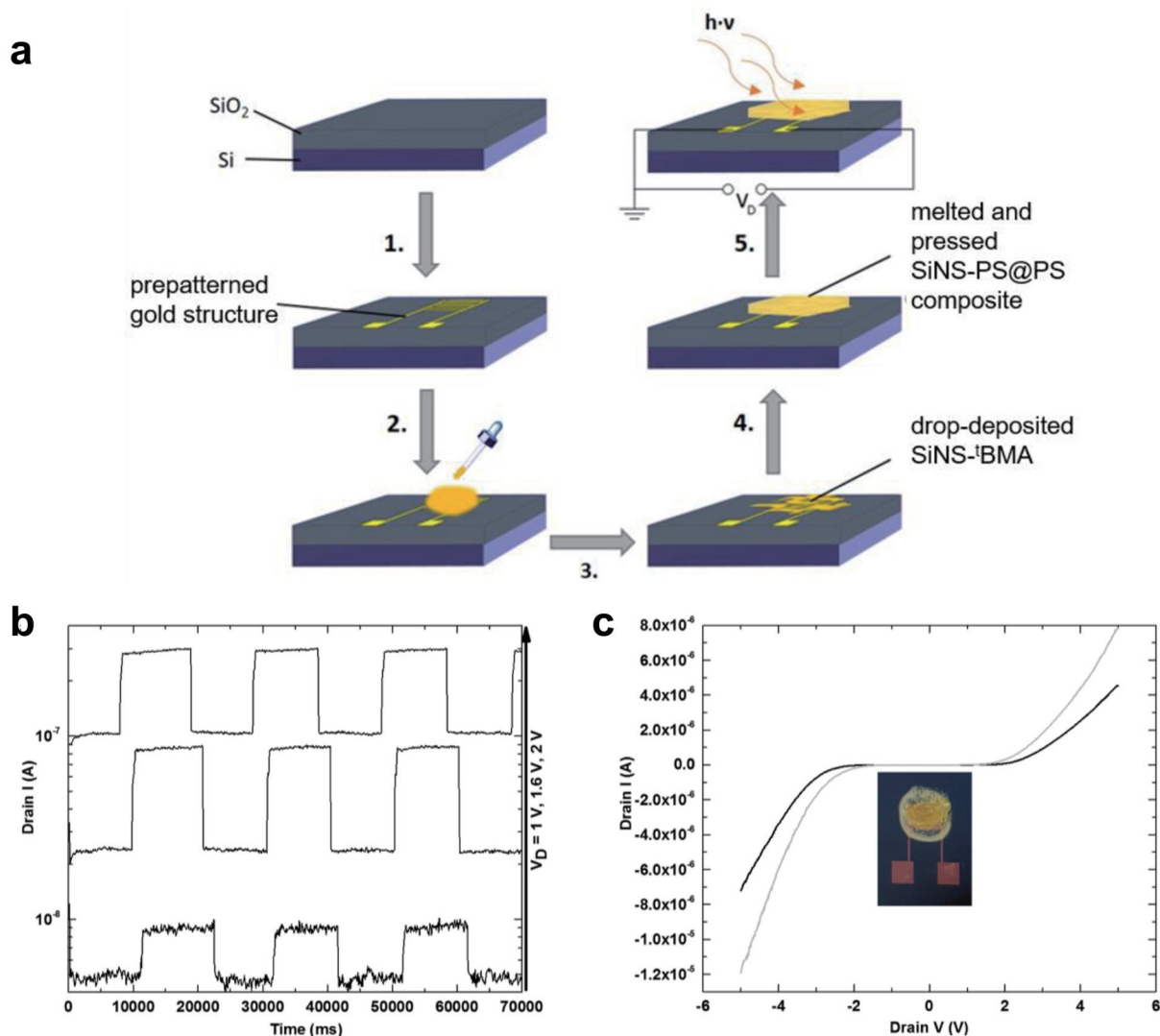


Fig. 8. (Color online) Preparation and photocurrent response of 2DSi-based devices. (a) Fabrication of photosensitive device based on silicene/polystyrene hybrids. (b, c) The plots of drain current versus time and drain current versus drain voltage of the devices fabricated following the procedures shown in (a). The inset in (c) shows a picture of the device setup under light irradiation. Reprinted with permission from Ref. [32]. Copyright 2017 by IOP Publishing Ltd.

duced from 2.31 to 2.13 eV^[95]. The significant red-shift of the absorption bandedge of silicene from ~ 520 to ~ 800 nm enabled the generation of photocurrent response under visible light irradiation (> 420 nm). Because of the anchoring of the densely packed benzyl group, the stability of the 2DSi structure was substantially enhanced. No decomposition of the silicene electrode was observed even after a 7-day immersion in the electrolyte solution.

The application of 2DSi/polymer homogenous hybrids as active materials for optoelectronic sensors has also been investigated^[32]. Polymerizable molecules, such as styrene and *tert*-butyl methacrylate (tBMA), have been applied to functionalized hydride-terminated silicene via radical-induced hydrosilylation, and were subsequently deposited on the metal electrodes via an airbrush-coating system (Fig. 8). An evident light-dependent change in drain current was observed as the photo-induced current increased exponentially toward higher and lower drain voltages once the absolute value of the drain voltages rose over 2 V.

5.3. (Photo)transistors

Many experimental studies have also been conducted on

the fabrication of 2DSi-based transistors. In 2015, Tao *et al.* fabricated the first proof-of-concept silicene-based FETs^[31]. Silicene was epitaxially grown on Ag(111)/mica substrate under UHV condition, encapsulated by Al_2O_3 , and transferred onto the SiO_2/Si substrate for contact deposition (Fig. 9). The manufacturing processes successfully stabilized silicene, so that the Raman and electrical signatures can last for ~ 2 min in air. The carrier mobility of ~ 100 $\text{cm}^2/(\text{V}\cdot\text{s})$ ($\mu_h = 99\text{--}129$ $\text{cm}^2/(\text{V}\cdot\text{s})$, $\mu_e = 58\text{--}86$ $\text{cm}^2/(\text{V}\cdot\text{s})$) was obtained from the non-degraded devices, which was believed to be attributed to the acoustic phonon-limited transport and grain boundary scattering. The differences in the charge carrier transport behaviors between single-layered and multilayered silicene were investigated by Grazianetti *et al.*^[47]. A similar encapsulation-free delamination method^[31] was applied on 2DSi samples with various layers of silicene (10 and 24 layers) to fabricate FETs. The multilayer silicene sample exhibited distinguished ambipolar behavior of the drain current at both sides of the branch bias. The measured charge neutrality point (i.e., the Dirac point V_D) ranged between 6 and 8 V with the current ON/OFF ratio up to 1.5 \times . The room-temperature field-effect mobilities of 10 lay-

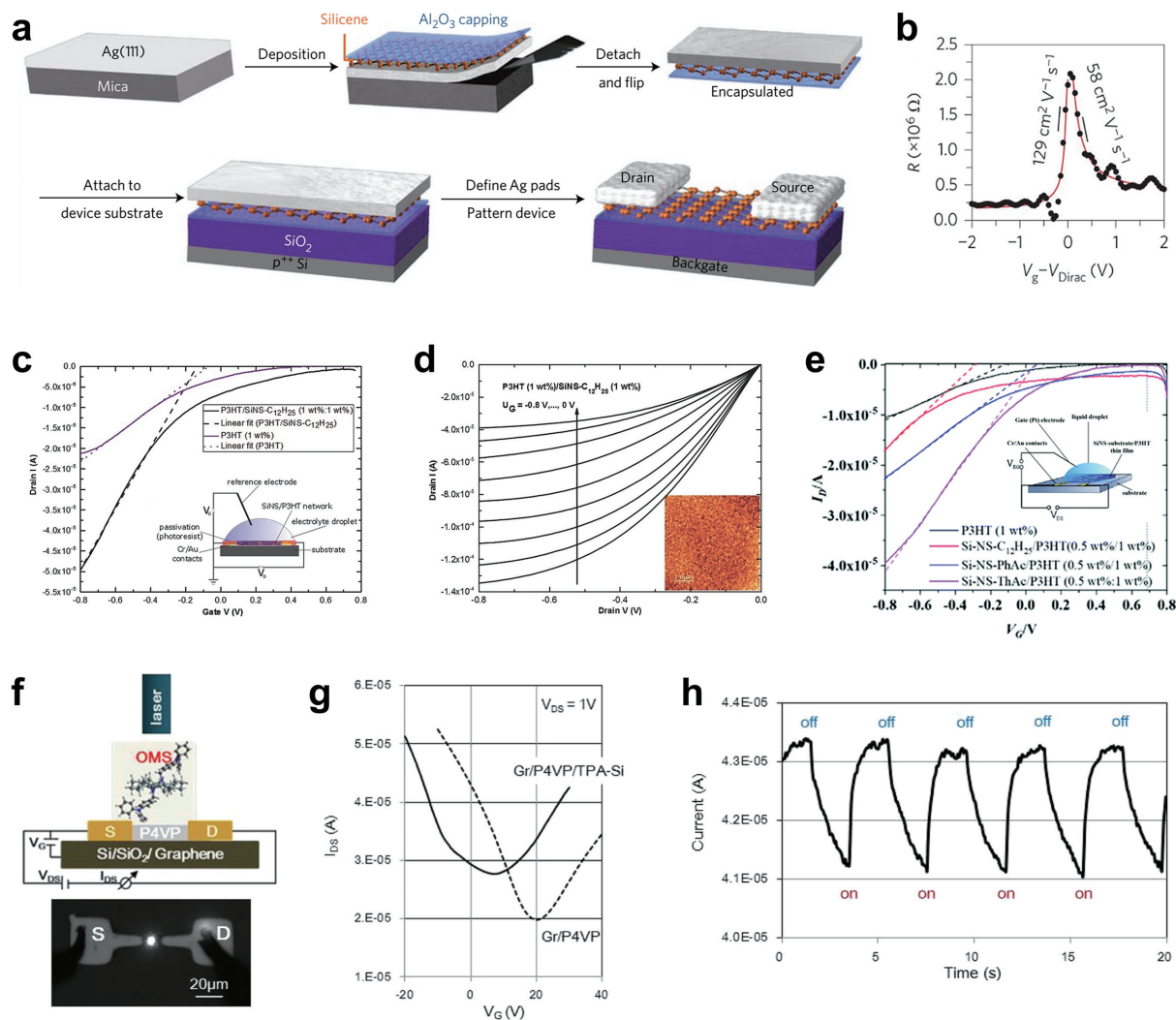


Fig. 9. (Color online) Device architectures and performance of 2DSi-based optoelectronics. (a) Schematic illustration of the fabrication processes of the first silicene-based transistors with highlighted key steps. (b) Corresponding R versus $V_g - V_{\text{Dirac}}$ plot of silicene transistor showing the device evidence of the Dirac-like band structure of silicene. Reprinted with permission from Ref. [31]. Copyright 2015 by Macmillan Publishers Limited. (c) Device performance of SGFET using the hybrid active material containing dodecyl-functionalized silicane ($\text{SiNS-C}_{12}\text{H}_{25}$) and P3HT polymer. Inset: the schematic of the device architecture. (d) Output drain current-voltage curves of the device shown in Fig. (c). Inset: AFM image of the active layer. Reprinted with permission from Ref. [93]. Copyright 2017 by Wiley-VCH. (e) Device performance of SGFET based on silicane functionalized with various types of ligands: dodecane ($\text{C}_{12}\text{H}_{25}$), phenylacetylene (PhAc), and 2-ethynyl-3-hexylthiophene (ThAc). The device architecture is shown in the inset figure. Reprinted with permission from Ref. [87]. Copyright 2018 by Royal Society of Chemistry. (f) Schematic (top) and optical image (bottom) of the device architecture of phototransistor based on organo-modified silicenes (OMS)/graphene hybrids. (g) Corresponding $I_{\text{DS}} - V_{\text{G}}$ curves of the devices with and without the presence of OMS. (h) Photocurrent response of the OMS/graphene hybrid phototransistors. Reprinted with permission from Ref. [107]. Copyright 2019 by Wiley-VCH.

ers and 24 layers of silicene were 66–200 and 49–63 $\text{cm}^2/(\text{V}\cdot\text{s})$, respectively, with a residual carrier density V_D of $\sim 10^{12} \text{ cm}^{-2}$, which were two orders of magnitude higher than that of the FETs using single-layer silicene as the active material. More importantly, these multilayered silicene FETs showed higher reproducible ambipolar response and improved stability (stable up to two days) than the single-layered silicene devices.

In addition to silicene, both silicane and MSNs have been used to fabricate thin-film transistors (TFTs). Helbich *et al.* functionalized hydride-terminated silicane with various unsaturated organic groups using hydrosilylation catalyzed by Lewis acids[93]. The functionalized silicanes exhibited improved materials stability and solution-processability and were capable of being blended with commercial semiconducting polymer poly(3-hexylthiophene-2,5-diyl) (P3HT) to construct solu-

tion-gated FETs (SGFETs). The devices operated at room temperature under ambient conditions with transconductances (g_m) of $7.45 \times 10^5 \text{ S}$. Compared to the control P3HT-only sample, devices with functionalized silicanes showed enhanced sensitivity and increased device transconductance by more than 100%. Lyuleeva *et al.* further optimized the silicane/polymer hybrids and directly functionalized silicane with thiophene-based ligands[87]. The direct functionalization with thiophene ligands improves the electronic transportation from the surface-modified silicane to P3HT via the polaron hopping processes from the P3HT polymer chain to the thiophene group. These devices had relatively low OFF currents and high ON currents, leading to an improved ON/OFF ratio of 8.3×10^2 .

Nakano *et al.* recently developed phototransistors using

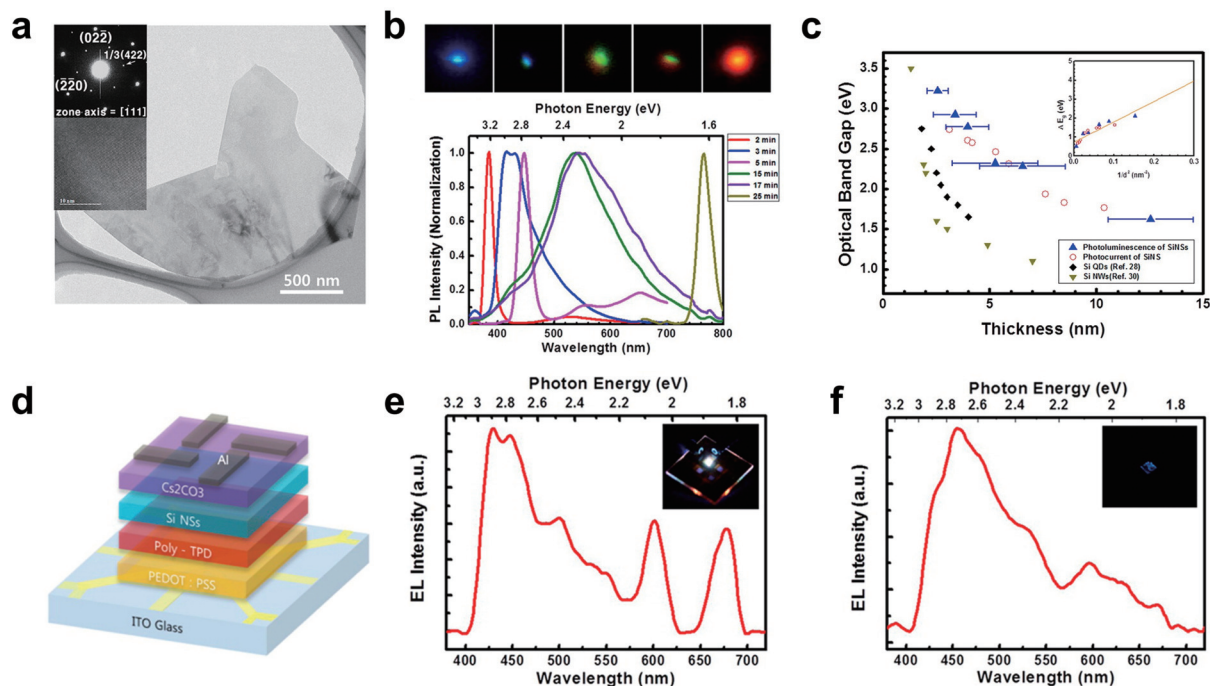


Fig. 10. (Color online) 2DSi-based LEDs. (a) Transmission electron microscopic images and corresponding diffraction pattern (inset) of MSNs used for LED application. (b) Real color images of the thickness-controlled MSNs with emission ranging from blue to red and corresponding PL spectra as a function of growth time. (c) Optical bandgap of MSNs as a function of the thickness determined from PL and photocurrent measurements. Inset: the optical bandgap as a function of thickness. (d) Schematic of the hybrid LEDs using MSNs as the active materials. (e) Electroluminescence (EL) spectrum of the MSN-based devices using mixed MSNs with various thicknesses. (f) EL spectrum of the SiNSs synthesized for a growth time of 5 min. Reprinted with permission from Ref. [30]. Copyright 2014 by American Chemical Society.

the silicene/graphene hybrids as the active materials^[107]. Hydride-terminated silicene was functionalized via dehydrogenation with arylmethylamine derivatives such as 4-(aminomethyl)quinoline (AM-Qu), 4-(aminomethyl)pyridine (AM-Py), and p-(aminomethyl)triphenylamine (AM-TPA). Computational studies confirmed that the highest occupied molecular orbital (HOMO) and the lowest unoccupied molecular orbital (LUMO) of passivated silicene were mainly contributed on the anchored organoamines and the silicon atoms, respectively. These features were believed to facilitate the photo-induced charge transfer from the ligands to the silicene backbone. The V_D of the TPA-Si/graphene hybrid phototransistors was 7 V, which was significantly smaller than those of pristine graphene ($V_D > 50$ V) and polymer-coated graphene devices ($V_D = 20$ V). Although the hole mobility was smaller than that of the silicene-based devices^[31], the phototransistors with amine-passivated silicenes show improved stability, which was attributed to the surface protection provided by the organic ligands.

5.4. Light-emitting applications

Differing from other quantum-confined materials (e.g., quantum dots) whose PL properties can be tailored through precise particle size control, the PL tuning of silicene can be achieved through surface modification. The green PL of hydride- or hydroxyl-terminated silicene may originate from the radiative recombination at the direct-bandgap-like bandedge^[27]. In contrast, the blue PL from the amine-functionalized silicene was attributed to the trap states created by the interaction with organoamines or oxide species^[56]. The PL quantum yield (PLQY) values of the existent silicenes are relatively low (usually below 10%) compared to their SiNC counter-

parts^[108]. For instance, Karar *et al.* reported that the PLQY of green-emitting quasi-two-dimensional silicon nanosheets (i.e., stacked, partially oxide-crosslinked silicenes) is 9%^[109]. A similar PLQY value was obtained from the hydride-/hydroxyl-terminated silicene^[27].

Single-layered silicene has garnered much interest due to its unique electrical and optical properties; however, the instability of the intrinsic materials under operating conditions precludes its use as the active materials for optoelectronics in many circumstances. However, the freestanding bilayer silicene (BSi) has been proven experimentally to have better stability and has been considered as an ideal material candidate for superconductors and topological insulators^[28, 29, 101, 110]. The potentials of BSi as active materials for optoelectronics were investigated using DFT calculations by Huang *et al.*^[111] The results indicate that the naked BSi has an indirect bandgap, which may not be suitable for optoelectronic applications, whereas the partially hydride-terminated BSi nanoclusters with the numbers of Si atoms below 28 show dipole-allowed direct (or quasi-direct) bandgaps with gaps between 1.01 and 2.85 eV. Three BSi structures (Si_8H_4 , $\text{Si}_{16}\text{H}_{12}$, and $\text{Si}_{12}\text{H}_{10}$) have been predicted to have direct (or quasi direct) with a range of the full visible regime, which can be used as the active materials for white-light LEDs.

The first 2DSi-based LED was reported by Kim *et al.* in 2014^[30]. Single-crystalline MSNs were grown through chemical vapor deposition using SiCl_4 as the silicon precursor under the H_2 atmosphere. By controlling the growth times ranging from 1.5 to 20 min, MSNs with various sizes were formed with PL across the visible to near-infrared region (from 385 to 765 nm). White-light emissions were also obtained by mixing

the MSNs prepared with different growth times. The authors further fabricated solution-processable LEDs with an MSN-based emissive layer (Fig. 10). The resulting white-light and blue-light electroluminescence (EL) spectra were consistent with the PL features of the corresponding MSNs, indicating that the EL originates from the radiative recombination of the charge carriers at the bandedge of MSNs.

6. Conclusion and perspectives

This review has outlined the recent progress relative to 2DSi nanomaterials, surface modification approaches, and the corresponding optoelectronic applications. As one of the important members in the family of nanomaterials, 2DSis have demonstrated encouraging electronic and optical properties, and the corresponding devices have advanced during the last decade. The intrinsic features of silicon, such as elemental abundance and high biocompatibility, further make 2DSi amenable to be applied in energy storage and conversion, biotechnology, and photonics.

Despite the recent success in 2DSi research, several critical issues must be addressed. The first issue concerns the scale-up synthesis of 2DSi materials with high crystalline quality. Although preparation approaches, such as epitaxial growth and chemical exfoliation, have been optimized for various types of 2DSi, we do not yet understand the growth mechanisms of 2DSi materials under certain reaction conditions. Thus, it is crucial to revisit and further optimize the synthesis routes of 2DSi, such as:

(1) To gain a better understanding of the growth mechanism behind the synthesis route, to determine the step reactions and the roles of silicon precursors, solvents, environments, reaction temperature and time;

(2) To precisely control the structure, size, and morphology of the product 2DSi and to analyze the physical and chemical properties of the product(s) and byproduct(s);

(3) To design and realize the potential internal transition of 2DSi materials, uncover the fine-tuning conditions such as reaction temperature and time, substrate, carrier gas or solvent, precursor ratio, and the type of catalyst.

Second, surface analysis and ligand engineering are crucial to 2DSi materials. The covalent nature of the silicon backbones in 2DSis differs from those of many other ionic nanomaterials. The “naked” sp²-hybridized silicon atoms on silicene and the as-formed hydride-terminated surfaces of silicane and MSNs are both prone to oxidation, which introduces trap states that may promote additional recombination pathways of charge carriers and thus impair the electronic properties. Although conventional surface modification approaches (such as hydrosilylation and Grignard reactions) have been widely used for functionalizing c-Si, differences exist when comparing the bond strength and steric hindrance of the silicon atoms on the surfaces on the bulky and nanoscaled silicon materials. Consequently, new functionalization methods that can circumvent the limitation of these existent methods are urgently needed to passivate 2DSis to gain better stability, more vigorous PL intensity, and high charge carrier mobilities.

Third, although considerable progress has been made on the understanding of the properties of 2DSis, the fabrication and optimization of 2DSi-based devices remain a significant

challenge. Although a few prototype devices (e.g., transistors, sensors, LEDs) have been reported, most of them suffer from materials and device instability and relatively low performance. Additional efforts have to be made to further boost the device performance and improve the device stability under the operational conditions. Coupling the materials with polymers^[32, 93] and the search for proper device architectures^[96] would be effective routes towards those goals. Meanwhile, the computational studies on the properties of new 2DSis (e.g., doping, alloy)^[112, 113] would accelerate the searching of new material candidates with better optoelectronic properties in the 2DSi family.

Although 2DSi materials have been found and studied since the nineteenth century, they still behave like newcomers in the fields of silicon-based science and engineering. Therefore, future studies on the synthesis and surface modification of 2DSis are crucial because they pave the way to deepen the understanding of the properties of these reduced-dimensional materials and to boost device performance.

Acknowledgements

The authors would like to acknowledge financial support from the National Natural Science Foundation of China (21905316, 22175201), Guangdong Natural Science Foundation (2019A1515011748), the Science and Technology Planning Project of Guangdong Province (2019A050510018), and Sun Yat-sen University.

References

- [1] Heersche H B, Jarillo-Herrero P, Oostinga J B, et al. Bipolar supercurrent in graphene. *Nature*, 2007, 446(7131), 56
- [2] Du X, Skachko I, Barker A, et al. Approaching ballistic transport in suspended graphene. *Nat Nanotechnol*, 2008, 3(8), 491
- [3] Wang F, Zhang Y, Tian C, et al. Gate-variable optical transitions in graphene. *Science*, 2008, 320(5873), 206
- [4] Lee C, Wei X, Kysar J W, et al. Measurement of the elastic properties and intrinsic strength of monolayer graphene. *Science*, 2008, 321(5887), 385
- [5] Scheuermann G M, Rumi L, Steurer P, et al. Palladium nanoparticles on graphite oxide and its functionalized graphene derivatives as highly active catalysts for the Suzuki–Miyaura Coupling reaction. *J Am Chem Soc*, 2009, 131(23), 8262
- [6] Lu Y, Lu Y, Niu Z, et al. Graphene-based nanomaterials for sodium-ion batteries. *Adv Energy Mater*, 2018, 8(17), 1702469
- [7] Lin L, Peng H, Liu Z. Synthesis challenges for graphene industry. *Nat Mater*, 2019, 18(6), 520
- [8] Deng X, Zheng X, Yuan T, et al. Ligand impact of silicenes as anode materials for lithium-ion batteries. *Chem Mater*, 2021, 33(23), 9357
- [9] Xu H, Chen H, Gao C. Advanced graphene materials for sodium/potassium/aluminum-ion batteries. *ACS Mater Lett*, 2021, 3(8), 1221
- [10] Wang Q H, Kalantar-Zadeh K, Kis A, et al. Electronics and optoelectronics of two-dimensional transition metal dichalcogenides. *Nat Nanotechnol*, 2012, 7(11), 699
- [11] Mak K F, Shan J. Photonics and optoelectronics of 2D semiconductor transition metal dichalcogenides. *Nat Photonics*, 2016, 10(4), 216
- [12] Meng J L, Wang T Y, Chen L, et al. Energy-efficient flexible photoelectric device with 2D/0D hybrid structure for bio-inspired artificial heterosynapse application. *Nano Energy*, 2021, 83, 105815
- [13] Meng J L, Wang T Y, He Z Y, et al. Flexible boron nitride-based

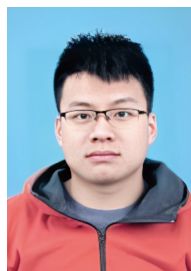
- memristor for in situ digital and analogue neuromorphic computing applications. *Mater Horiz*, 2021, 8(2), 538
- [14] Wang C, Xu X, Pi X, et al. Neuromorphic device based on silicon nanosheets. *Nat Commun*, 2022, 13(1), 5216
- [15] Meng J, Wang T, Zhu H, et al. Integrated in-sensor computing optoelectronic device for environment-adaptable artificial retina perception application. *Nano Lett*, 2022, 22(1), 81
- [16] Cahangirov S, Topsakal M, Aktürk E, et al. Two- and one-dimensional honeycomb structures of silicon and germanium. *Phys Rev Lett*, 2009, 102(23), 236804
- [17] Guzmán-Verri G G, Lew Yan Voon L C. Electronic structure of silicon-based nanostructures. *Phys Rev B*, 2007, 76(7), 075131
- [18] Morishita T, Russo S P, Snook I K, et al. First-principles study of structural and electronic properties of ultrathin silicon nanosheets. *Phys Rev B*, 2010, 82(4), 045419
- [19] Liu C C, Feng W, Yao Y. Quantum spin Hall effect in silicene and two-dimensional germanium. *Phys Rev Lett*, 2011, 107(7), 076802
- [20] Spencer M J S, Morishita T, Snook I K. Reconstruction and electronic properties of silicon nanosheets as a function of thickness. *Nanoscale*, 2012, 4(9), 2906
- [21] Chigo Anotá E, Bautista Hernández A, Castro M, et al. Investigating the electronic properties of silicon nanosheets by first-principles calculations. *J Mol Model*, 2012, 18(5), 2147
- [22] Kamal C, Chakrabarti A, Banerjee A, et al. Silicene beyond monolayers—different stacking configurations and their properties. *J Physics: Condens Matter*, 2013, 25(8), 085508
- [23] Gao J, Zhang J, Liu H, et al. Structures, mobilities, electronic and magnetic properties of point defects in silicene. *Nanoscale*, 2013, 5(20), 9785
- [24] Li S, Wu Y, Liu W, et al. Control of band structure of van der Waals heterostructures: Silicene on ultrathin silicon nanosheets. *Chem Phys Lett*, 2014, 609, 161
- [25] Roman R E, Cranford S W. Mechanical properties of silicene. *Comput Mater Sci*, 2014, 82, 50
- [26] Quhe R, Fei R, Liu Q, et al. Tunable and sizable band gap in silicene by surface adsorption. *Sci Rep*, 2012, 2(1), 853
- [27] Ryan B J, Hanrahan M P, Wang Y, et al. Silicene, siloxene, or silicane? Revealing the structure and optical properties of silicon nanosheets derived from calcium disilicide. *Chem Mater*, 2020, 32(2), 795
- [28] De Padova P, Kubo O, Olivieri B, et al. Multilayer silicene nanoribbons. *Nano Lett*, 2012, 12(11), 5500
- [29] Feng B, Ding Z, Meng S, et al. Evidence of silicene in honeycomb structures of silicon on Ag(111). *Nano Lett*, 2012, 12(7), 3507
- [30] Kim S W, Lee J, Sung J H, et al. Two-dimensionally grown single-crystal silicon nanosheets with tunable visible-light emissions. *ACS Nano*, 2014, 8(7), 6556
- [31] Tao L, Cinquanta E, Chiappe D, et al. Silicene field-effect transistors operating at room temperature. *Nat Nanotechnol*, 2015, 10(3), 227
- [32] Lyuleeva A, Helbich T, Rieger B, et al. Polymer-silicon nanosheet composites: bridging the way to optoelectronic applications. *J Phys D*, 2017, 50(13), 135106
- [33] Berger C, Song Z, Li T, et al. Ultrathin epitaxial graphite: 2D electron gas properties and a route toward graphene-based nanoelectronics. *J Phys Chem B*, 2004, 108(52), 19912
- [34] Sutter P W, Flege J I, Sutter E A. Epitaxial graphene on ruthenium. *Nat Mater*, 2008, 7(5), 406
- [35] Hao R, Qian W, Zhang L, et al. Aqueous dispersions of TCNQ-anion-stabilized graphene sheets. *Chem Commun*, 2008, 48, 6576
- [36] Novoselov K S, Jiang D, Schedin F, et al. Two-dimensional atomic crystals. *Proceedings of the National Academy of Sciences of the United States of America*, 2005, 102(30), 10451
- [37] Wöhler F. Ueber verbindungen des siliciums mit sauerstoff und wasserstoff. *Justus Liebigs Annalen der Chemie*, 1863, 127(3), 257
- [38] Weiss A, Beil G, Meyer H. The topochemical reaction of CaSi_2 to a two-dimensional subsiliceous acid $\text{Si}_6\text{H}_3(\text{OH})_3$ (= Kautsky' Siloxene). *J Zeitschrift für Naturforschung B*, 1980, 35, 25
- [39] Dahn J R, Way B M, Fuller E, et al. Structure of siloxene and layered polysilane (Si_6H_6). *Phys Rev B*, 1993, 48(24), 17872
- [40] Min H, Hill J E, Sinitsyn N A, et al. Intrinsic and Rashba spin-orbit interactions in graphene sheets. *Phys Rev B*, 2006, 74(16), 165310
- [41] Ezawa M. A topological insulator and helical zero mode in silicene under an inhomogeneous electric field. *New J Phys*, 2012, 14(3), 033003
- [42] Liu J, Yang Y, Lyu P, et al. Few-layer silicene nanosheets with superior lithium-storage properties. *Adv Mater*, 2018, 30(26), 1800838
- [43] Linti G. Silicon chemistry. From the Atom to Extended Systems. Edited by Peter Jutzi and Ulrich Schubert. *Angew Chem Int Ed*, 2004, 43(23), 135
- [44] Okamoto H, Kumai Y, Sugiyama Y, et al. Silicon nanosheets and their self-assembled regular stacking structure. *J Am Chem Soc*, 2010, 132(8), 2710
- [45] Li F, Lu R, Yao Q, et al. Geometric and electronic structures as well as thermodynamic stability of hexyl-modified silicon nanosheet. *J Phys Chem C*, 2013, 117(25), 13283
- [46] De Padova P, Generosi A, Paci B, et al. Multilayer silicene: clear evidence. *2D Mater*, 2016, 3(3), 031011
- [47] Grazianetti C, Cinquanta E, Tao L, et al. Silicon nanosheets: Crossover between multilayer silicene and diamond-like growth regime. *ACS Nano*, 2017, 11(3), 3376
- [48] Chen H D, Chien K H, Lin C Y, et al. Few-layer silicon films on the Ag(111) surface. *J Phys Chem C*, 2016, 120(5), 2698
- [49] Padova P D, Generosi A, Paci B, et al. Corrigendum: Multilayer silicene: clear evidence. *2D Mater*, 2016, 3(4), 049501
- [50] Okamoto H, Sugiyama Y, Nakano H. Synthesis and modification of silicon nanosheets and other silicon nanomaterials. *Chem Eur J*, 2011, 17(36), 9864
- [51] Chen J, Du Y, Li Z, et al. Delocalized surface state in epitaxial Si(111) film with spontaneous $\sqrt{3} \times \sqrt{3}$ superstructure. *Sci Rep*, 2015, 5(1), 13590
- [52] Chen L, Liu C C, Feng B, et al. Evidence for Dirac fermions in a honeycomb lattice based on silicon. *Phys Rev Lett*, 2012, 109(5), 056804
- [53] De Padova P, Vogt P, Resta A, et al. Evidence of Dirac fermions in multilayer silicene. *Appl Phys Lett*, 2013, 102(16), 163106
- [54] Hwang G C, Blom D A, Vogt T, et al. Pressure-driven phase transitions and reduction of dimensionality in 2D silicon nanosheets. *Nat Commun*, 2018, 9(1), 5412
- [55] Nakano H. Synthesis and modification of two-dimensional crystalline silicon nanosheets. *J Ceram Soc Jpn*, 2014, 122(1429), 748
- [56] Nakano H, Ikuno T. Soft chemical synthesis of silicon nanosheets and their applications. *Appl Phys Rev*, 2016, 3(4), 040803
- [57] Yu X, Xue F, Huang H, et al. Synthesis and electrochemical properties of silicon nanosheets by DC arc discharge for lithium-ion batteries. *Nanoscale*, 2014, 6(12), 6860
- [58] Ryu J, Chen T, Bok T, et al. Mechanical mismatch-driven rippling in carbon-coated silicon sheets for stress-resilient battery anodes. *Nat Commun*, 2018, 9(1), 2924
- [59] Lalmi B, Oughaddou H, Enriquez H, et al. Epitaxial growth of a silicene sheet. *Appl Phys Lett*, 2010, 97(22), 223109
- [60] Meng L, Wang Y, Zhang L, et al. Buckled silicene formation on Ir(111). *Nano Lett*, 2013, 13(2), 685
- [61] Fleurence A, Friedlein R, Ozaki T, et al. Experimental evidence for epitaxial silicene on diboride thin films. *Phys Rev Lett*, 2012, 108(24), 245501
- [62] Warner J H, Rummeli M H, Bachmatiuk A, et al. Atomic resolution imaging and topography of boron nitride sheets produced

- by chemical exfoliation. *ACS Nano*, 2010, 4(3), 1299
- [63] Xu J, Zhang L, Shi R, et al. Chemical exfoliation of graphitic carbon nitride for efficient heterogeneous photocatalysis. *J Mater Chem A*, 2013, 1(46), 14766
- [64] Ding Y, Chen Y P, Zhang X, et al. Controlled intercalation and chemical exfoliation of layered metal–organic frameworks using a chemically labile intercalating agent. *J Am Chem Soc*, 2017, 139(27), 9136
- [65] Yamanaka S, Matsu-ura H, Ishikawa M. New deintercalation reaction of calcium from calcium disilicide. Synthesis of layered polysilane. *Mater Res Bull*, 1996, 31(3), 307
- [66] Nakano H, Mitsuoka T, Harada M, et al. Soft synthesis of single-crystal silicon monolayer sheets. *Angew Chem Int Ed*, 2006, 45(38), 6303
- [67] Lang J, Ding B, Zhang S, et al. Scalable synthesis of 2D Si nanosheets. *Adv Mater*, 2017, 29(31), 1701777
- [68] Qiu J, Fu H, Xu Y, et al. From silicene to half-silicane by hydrogenation. *ACS Nano*, 2015, 9(11), 11192
- [69] Wang W, Olovsson W, Uhrberg R I G. Band structure of hydrogenated silicene on Ag(111): Evidence for half-silicane. *Phys Rev B*, 2016, 93(8), 081406
- [70] Liao W S, Lee S C. Water-induced room-temperature oxidation of Si–H and –Si–Si– bonds in silicon oxide. *J Appl Phys*, 1996, 80(2), 1171
- [71] Pereira R N, Rowe D J, Anthony R J, et al. Oxidation of freestanding silicon nanocrystals probed with electron spin resonance of interfacial dangling bonds. *Phys Rev B*, 2011, 83(15), 155327
- [72] Acun A, Poelsema B, Zandvliet H J W, et al. The instability of silicene on Ag(111). *Appl Phys Lett*, 2013, 103(26), 263119
- [73] Cottrell T L. The strengths of chemical bonds. Butterworths Scientific, 1958
- [74] Song J H, Sailor M J. Dimethyl sulfoxide as a mild oxidizing agent for porous silicon and its effect on photoluminescence. *Inorg Chem*, 1998, 37(13), 3355
- [75] Dasog M, Yang Z, Regli S, et al. Chemical insight into the origin of red and blue photoluminescence arising from freestanding silicon nanocrystals. *ACS Nano*, 2013, 7(3), 2676
- [76] Ohshita J, Yamamoto K, Tanaka D, et al. Preparation and photocurrent generation of silicon nanosheets with aromatic substituents on the surface. *J Phys Chem C*, 2016, 120(20), 10991
- [77] Helbich T, Lyuleeva A, Ludwig T, et al. One-step synthesis of photoluminescent covalent polymeric nanocomposites from 2D silicon nanosheets. *Adv Funct Mater*, 2016, 26(37), 6711
- [78] Linford M R, Chidsey C E D. Alkyl monolayers covalently bonded to silicon surfaces. *J Am Chem Soc*, 1993, 115(26), 12631
- [79] Terry J, Linford M R, Wigren C, et al. Determination of the bonding of alkyl monolayers to the Si(111) surface using chemical-shift, scanned-energy photoelectron diffraction. *Appl Phys Lett*, 1997, 71(8), 1056
- [80] Terry J, Linford M R, Wigren C, et al. Alkyl-terminated Si(111) surfaces: A high-resolution, core level photoelectron spectroscopy study. *J Appl Phys*, 1998, 85(1), 213
- [81] Effenberger F, Götz G, Bidlingmaier B, et al. Photoactivated preparation and patterning of self-assembled monolayers with 1-alkenes and aldehydes on silicon hydride surfaces. *Angew Chem Int Ed*, 1998, 37(18), 2462
- [82] Cicero R L, Linford M R, Chidsey C E D. Photoreactivity of unsaturated compounds with hydrogen-terminated silicon(111). *Langmuir*, 2000, 16(13), 5688
- [83] Stewart M P, Buriak J M. Exciton-mediated hydrosilylation on photoluminescent nanocrystalline silicon. *J Am Chem Soc*, 2001, 123(32), 7821
- [84] Eves B J, Lopinski G P. Formation of organic monolayers on silicon via gas-phase photochemical reactions. *Langmuir*, 2006, 22(7), 3180
- [85] Wang X, Ruther R E, Streifer J A, et al. UV-induced grafting of alkenes to silicon surfaces: Photoemission versus excitons. *J Am Chem Soc*, 2010, 132(12), 4048
- [86] Helbich T, Lyuleeva A, Höhlein I M D, et al. Radical-induced hydrosilylation reactions for the functionalization of two-dimensional hydride terminated silicon nanosheets. *Chem Eur J*, 2016, 22(18), 6194
- [87] Lyuleeva A, Holzmüller P, Helbich T, et al. Charge transfer doping in functionalized silicon nanosheets/P3HT hybrid material for applications in electrolyte-gated field-effect transistors. *J Mater Chem C*, 2018, 6(27), 7343
- [88] Helbich T, Kloberg M J, Sinelnikov R, et al. Diaryliodonium salts as hydrosilylation initiators for the surface functionalization of silicon nanomaterials and their collaborative effect as ring opening polymerization initiators. *Nanoscale*, 2017, 9(23), 7739
- [89] Kloberg M J, Helbich T, Rieger B. Silicon nanosheets as co-initiators for diaryliodonium induced radical and cationic polymerization. *Nanotechnology*, 2018, 30(7), 075602
- [90] Sudo T, Asao N, Gevorgyan V, et al. Lewis acid catalyzed highly regio- and stereocontrolled trans-hydrosilylation of alkynes and alkenes. *J Org Chem*, 1999, 64(7), 2494
- [91] Buriak J M, Allen M J. Lewis acid mediated functionalization of porous silicon with substituted alkenes and alkynes. *J Am Chem Soc*, 1998, 120(6), 1339
- [92] Purkait T K, Iqbal M, Wahl M H, et al. Borane-catalyzed room-temperature hydrosilylation of alkenes/alkynes on silicon nanocrystal surfaces. *J Am Chem Soc*, 2014, 136(52), 17914
- [93] Helbich T, Lyuleeva A, Marx P, et al. Lewis acid induced functionalization of photoluminescent 2D silicon nanosheets for the fabrication of functional hybrid films. *Adv Funct Mater*, 2017, 27(21), 1606764
- [94] Sugiyama Y, Okamoto H, Mitsuoka T, et al. Synthesis and optical properties of monolayer organosilicon nanosheets. *J Am Chem Soc*, 2010, 132(17), 5946
- [95] Ohashi M, Shirai S, Nakano H. Direct chemical synthesis of benzyl-modified silicane from calcium disilicide. *Chem Mater*, 2019, 31(13), 4720
- [96] Kumai Y, Kadoura H, Sudo E, et al. Si–C composite anode of layered polysilane (Si₆H₆) and sucrose for lithium ion rechargeable batteries. *J Mater Chem*, 2011, 21(32), 11941
- [97] Sun L, Wang B, Wang Y. A novel silicon carbide nanosheet for high-performance humidity sensor. *Adv Mater Interfaces*, 2018, 5(6), 1701300
- [98] Lyuleeva A, Helbich T, Bobinger M, et al. Functionalized and oxidized silicon nanosheets: Customized design for enhanced sensitivity towards relative humidity. *Sens Actuators B*, 2019, 283, 451
- [99] Ryu J, Jang Y J, Choi S, et al. All-in-one synthesis of mesoporous silicon nanosheets from natural clay and their applicability to hydrogen evolution. *NPG Asia Mater*, 2016, 8(3), e248
- [100] Wang S, Wang C, Pan W, et al. Two-dimensional silicon for (photo)catalysis. *Sol RRL*, 2020, 2000392
- [101] Liu F, Liu C C, Wu K, et al. d+id' chiral superconductivity in bilayer silicene. *Phys Rev Lett*, 2013, 111(6), 066804
- [102] Ezawa M. Valley-polarized metals and quantum anomalous Hall effect in silicene. *Phys Rev Lett*, 2012, 109(5), 055502
- [103] Li X, Mullen J T, Jin Z, et al. Intrinsic electrical transport properties of monolayer silicene and MoS₂ from first principles. *Phys Rev B*, 2013, 87(11), 115418
- [104] Ding Y, Wang Y. Electronic structures of silicene fluoride and hydride. *Appl Phys Lett*, 2012, 100(8), 083102
- [105] Wang R, Pi X, Ni Z, et al. Density functional theory study on organically surface-modified silicene. *RSC Adv*, 2015, 5(43), 33831
- [106] Ni Z, Liu Q, Tang K, et al. Tunable bandgap in silicene and germanene. *Nano Lett*, 2012, 12(1), 113
- [107] Nakano H, Tanaka Y, Yamamoto K, et al. Silicanes modified by conjugated substituents for optoelectronic devices. *Adv Opt Mater*,

- 2019, 7(18), 1900696
- [108] Dasog M, Kehrle J, Rieger B, et al. Silicon nanocrystals and silicon-polymer hybrids: Synthesis, surface engineering, and applications. *Angew Chem Int Ed*, 2016, 55(7), 2322
- [109] Karar D, Bandyopadhyay N R, Pramanick A K, et al. Quasi-two-dimensional luminescent silicon nanosheets. *J Phys Chem C*, 2018, 122(33), 18912
- [110] Ezawa M. Quasi-topological insulator and trigonal warping in gated bilayer silicene. *J Phys Soc Jpn*, 2012, 81(10), 104713
- [111] Huang B, Deng H X, Lee H, et al. Exceptional optoelectronic properties of hydrogenated bilayer silicene. *Phys Rev X*, 2014, 4(2), 021029
- [112] Hussain T, Chakraborty S, Ahuja R. Metal-functionalized silicene for efficient hydrogen storage. *ChemPhysChem*, 2013, 14(15), 3463
- [113] Pi X, Ni Z, Liu Y, et al. Density functional theory study on boron- and phosphorus-doped hydrogen-passivated silicene. *Phys Chem Chem Phys*, 2015, 17(6), 4146



Xuebiao Deng received his bachelor's degree from the School of Chemistry at Sun Yat-sen University in 2019. He is currently a Ph.D. candidate supervised by Professor Zhenyu Yang at Sun Yat-sen University. His research has focused on the synthesis and applications of two-dimensional silicon and germanium nanostructures.



Huai Chen earned his Ph.D. in Chemistry from Sun Yat-sen University in 2022. He has been working on his postdoctoral research at the School of Chemistry, Sun Yat-sen University. His current research interest includes silicon-based nanomaterials for biomedical and optoelectronic applications.



Zhenyu Yang received his B.Sc. degree in Chemistry from Nankai University in 2009 and his Ph.D. degree in Chemistry from the University of Alberta in 2014. From 2014 to 2018, he was a postdoctoral researcher at the University of Toronto. In 2018, he joined the School of Chemistry at Sun Yat-sen University as a Professor. His research focuses on the development of solution-processible optoelectronic materials and devices.